Waves in turbulent stably-stratified shear flow

By F. G. Jacobitz †, M. M. Rogers ‡ AND J. H. Ferziger ¶

Two approaches for the identification of internal gravity waves in sheared and unsheared homogeneous stratified turbulence are investigated. First, the phase angle between the vertical velocity and density fluctuations is considered. It is found, however, that a continuous distribution of the phase angle is present in weakly and strongly stratified flow. Second, a projection onto the solution of the linearized inviscid equations of motion of unsheared stratified flow is investigated. It is found that a solution of the fully nonlinear viscous Navier-Stokes equations can be represented by the linearized inviscid solution. The projection yields a decomposition into vertical wave modes and horizontal vortical modes.

1. Introduction

An important problem in geophysical fluid mechanics is the characterization of turbulence and wave motion in stably-stratified flows. Fluid motion can occur as a result of either of these phenomena, and the ability to separate the motions associated with each should lead to better understanding and predictability of the flow. Stewart (1969) listed criteria that might be used to distinguish between internal wave motion and turbulence. The first distinction noted was that wave motion satisfies linear equations, whereas turbulence is inherently nonlinear. However, when both waves and turbulence are present, the motions are coupled nonlinearly and it is unclear how to extract the wave component of the flow. Secondly, the processes by which energy is transported are different. In turbulence, energy is advected at the speed of the motion, whereas waves transport energy via pressure-velocity correlations, usually at a group velocity that is greater than the particle velocity. Lastly, Stewart noted the difference between turbulence and waves with regard to mixing. Except when they break, waves do not produce mixing. Although they can transport momentum, they cannot transport scalars. Thus the scalar flux $\overline{u_2\rho}$, where u_2 is the vertical velocity component, should be large in regions dominated by turbulence and small where waves predominate. Furthermore, the relative phase of vertical velocity fluctuations u_2 and density fluctuations ρ is different for waves and turbulence. For stably-stratified flows, in-phase motion between u_2 and ρ corresponds to down-gradient turbulent transport, while 180° out-of-phase motion is associated with counter-gradient turbulent transport. For wave motions, u_2 and ρ have a phase difference of 90° and there is no mean correlation between them.

Stewart (1969) concluded that this last distinction held the greatest promise for distinguishing waves and turbulence and this criterion has been used extensively ever since. For example, Stillinger, Helland, & Van Atta (1983) felt that their unsheared stably-stratified decaying turbulence "had been completely converted to random internal wave motions" when $\overline{u_2\rho}$ became zero. However, Lienhard & Van Atta (1990) pointed out that $\overline{u_2\rho}$ can be zero as a result of co-gradient and counter-gradient fluxes at different scales of motion

† University of California, Riverside
‡ NASA Ames Research Center
¶ Stanford University

cancelling each other out. More careful diagnosis requires examination of the cospectrum of $\overline{u_2\rho}$ as a function of wavenumber, as originally proposed by Stewart (1969). Defining the cospectrum Co and quadrature spectrum Qu as

$$Co_{u_2\rho}(k_1, x_2) = Re\left(\Sigma_{k_3}\tilde{u}_2^*(k_1, x_2, k_3)\tilde{\rho}(k_1, x_2, k_3)\right) \tag{1.1}$$

$$Qu_{u_2\rho}(k_1, x_2) = Im\left(\Sigma_{k_3}\tilde{u}_2^*(k_1, x_2, k_3)\tilde{\rho}(k_1, x_2, k_3)\right) \ , \tag{1.2}$$

where the tildes indicate Fourier transformed quantities, the phase angle $\phi_{u_2\rho}$ between vertical velocity u_2 and density ρ is given by

$$\phi_{u_2\rho} = \arctan\left(\frac{Qu_{u_2\rho}}{Co_{u_2\rho}}\right) \ . \tag{1.3}$$

The above spectral quantities (or similar measures in terms of other wavenumber components) have been used in evaluating both experimental and computational data on stratified flows. McBean & Miyake (1972) used measurements in the atmospheric surface layer to tentatively conclude that wave motions may be important at low frequencies in stably stratified flow. Komori, Ueda, Ogino & Mizushina (1983) felt that a significant fraction of the motion in their stably stratified open-channel flow experiment was wavelike based on the phase angles measured. In contrast, data from experiments in both unsheared (Lienhard & Van Atta 1990) and sheared (Piccirillo & Van Atta 1997) stably stratified homogeneous turbulence indicate no evidence of wavelike motion based on examination of the phase angle. Analysis of direct numerical simulations of similar sheared homogeneous stratified turbulence (Holt, Koseff & Ferziger 1992) also indicates that even for strong stratification there is no band of wavenumbers with $\phi_{u_2\rho} \approx 90°$.

Riley, Metcalfe, and Weissman (1981) proposed a different method for separating wavelike and turbulent motions. They used the Craya (1958) decomposition to split the turbulent velocity field associated with each wavenumber into two solenoidal components, one normal to the wavenumber vector and to the gravity vector, and the other orthogonal to the first component and to the wavenumber vector. For small amplitudes, this second component satisfies the linear propagation equation for internal gravity waves, and is thus identified as the "wave" component of the motion. The other component consists of quasi-horizontal motions containing all the vertical vorticity and is identified as "turbulence". This decomposition splits the flow into propagating and non-propagating parts only in the limit of zero Froude number. For small but finite Froude number Staquet and Riley (1989) proposed a generalization of this decomposition using Ertel's (1942) Theorem for potential vorticity. However, this generalization is invalid when the density gradient is zero or unbounded, and therefore cannot be used for turbulent flows.

Despite this shortcoming, Herring and Métais (1989) and Métais and Herring (1989) used the original Riley *et al.* decomposition to split their numerically-simulated turbulent flow fields into "wave" and "turbulent" components. They acknowledge the deficiencies of this approximation, noting 1) that "a proper definition of waves should include the density field, and its phase relative to the 'wave'-component of the velocity" and 2) their non-zero Froude number. However, the "turbulent" components of their flows do not show oscillations that scale with the Brunt–Väisälä frequency; such oscillations are observed in the wave component of the flows. This suggests a weak interaction between the components, and perhaps the adequacy of the decomposition.

The prototypical example of homogeneous turbulent stratified shear flow with uniform stable vertical stratification $S_\rho = \partial\rho/\partial x_2$ and uniform vertical shear $S = \partial U/\partial x_2$ is the simplest flow that contains both shear and stratification. It has been studied extensively

in the past due to its geophysical significance. Experimental investigations include Rohr, Itsweire, Helland & Van Atta (1988) and Piccirillo & Van Atta (1997). Numerical simulations include the work by Gerz, Schumann & Elghobashi (1989), Holt, Koseff & Ferziger (1992), Jacobitz, Sarkar & Van Atta (1997), Jacobitz (2000) and Shah, Koseff & Ferziger (2000). Turbulence in decaying stratified turbulence without shear has been investigated by Métais & Herring (1989), Lienhard & Van Atta (1990), Yoon & Warhaft (1990) and Briggs, Ferziger, Koseff & Monismith (1998).

In this study, possible ways to decompose the fluid motion into turbulence and wave components are investigated in direct numerical simulations of both sheared and unsheared homogeneous stratified turbulence. Both the phase angle between the vertical velocity and density and projections onto eigensolutions of the linearized governing equations are examined.

In the following section, the numerical simulations used in the present study are introduced. In sections 3 and 4, the phase angle results in sheared and unsheared stably stratified turbulence are presented. In section 5, a turbulence-wave decomposition based on the linear inviscid equations of motion is applied to the numerical data. Results are summarized in section 6.

2. The numerical simulations

The current study is based on the results of five direct numerical simulations of sheared, homogeneous stably-stratified turbulence and two direct numerical simulations of unsheared, decaying homogeneous stably-stratified turbulence.

In the direct numerical simulations, all dynamically-important scales of the velocity, density and pressure fields are resolved and no turbulence models are introduced. A spatial discretization is first performed to obtain a semi-discrete system of ordinary differential equations from the original system of partial differential equations. An integration of the system of ordinary differential equations is then performed to advance the solution in time. The spatial discretization is accomplished by a spectral collocation method. The temporal advancement is accomplished by a fourth-order Runge-Kutta scheme. A computational grid overlaying a cube of length 2π was used with 256^3 points. The initial conditions are taken from a separate simulation of isotropic turbulence without density fluctuations, which was allowed to develop for approximately one eddy turnover time. The energy spectrum of the initial field peaks at a wavenumber $k = 13$ and the resulting vertical integral scale, computed as the vertical integral of the autocorrelation of the vertical velocity component, is $L = 0.174$, compared to the box size 2π. The initial value of the Taylor microscale Reynolds number is taken as $Re_\lambda = 45$ in all simulations.

Figure 1 shows the evolution of the normalized turbulent kinetic energy K/K_0 for sheared stably-stratified turbulence with Richardson numbers $Ri = 0$, $Ri = 0.1$, $Ri = 0.2$, $Ri = 0.5$, and $Ri = 1.0$. Here the Richardson number is given by N^2/S^2, where N is the Brunt-Väisälä frequency, given by $\sqrt{(-g/\rho_0)\partial\overline{\rho}/\partial y}$. Initially, the turbulent kinetic energy decays as a result of the absence of Reynolds shear stress $\overline{u_1 u_2}$ in the isotropic initial condition. For simulations with small values of the Richardson number, the turbulent kinetic energy eventually grows with nondimensional time St. For simulations with large values of the Richardson number, however, the turbulent kinetic energy continues to decay, with the stratification overwhelming the turbulence production by the mean shear.

Figure 2 shows the evolution of the normalized turbulent kinetic energy K/K_0 for unsheared stably stratified turbulence with initial Froude numbers $Fr = 64$ and $Fr = 6.4$,

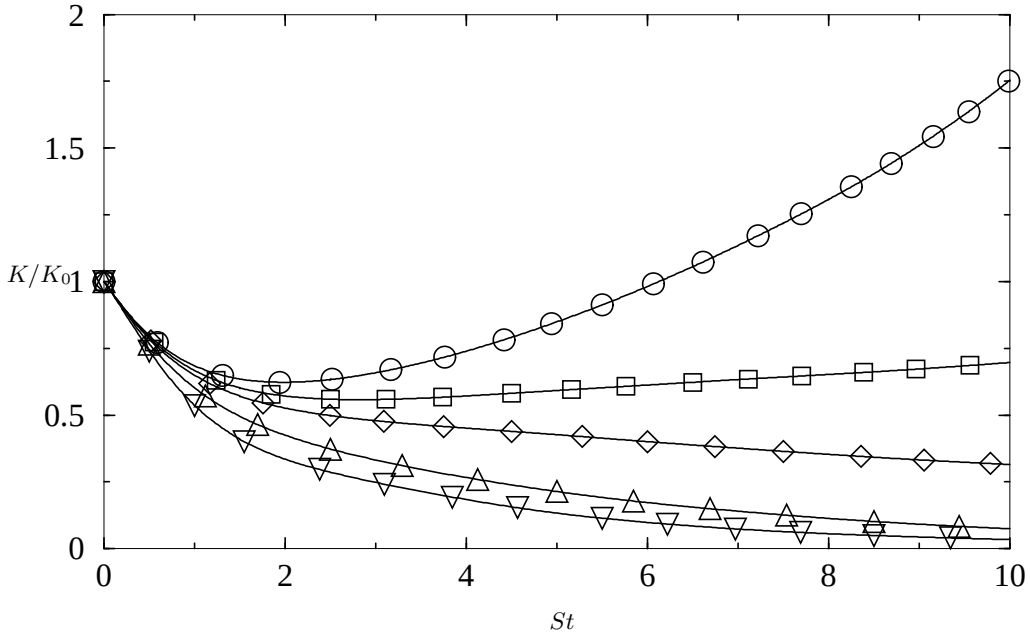

FIGURE 1. Evolution of the normalized turbulent kinetic energy K/K_0 in sheared stratified turbulence with Richardson numbers 0 (○), 0.1 (□), 0.2 (◇), 0.5 (△), and 1.0 (▽).

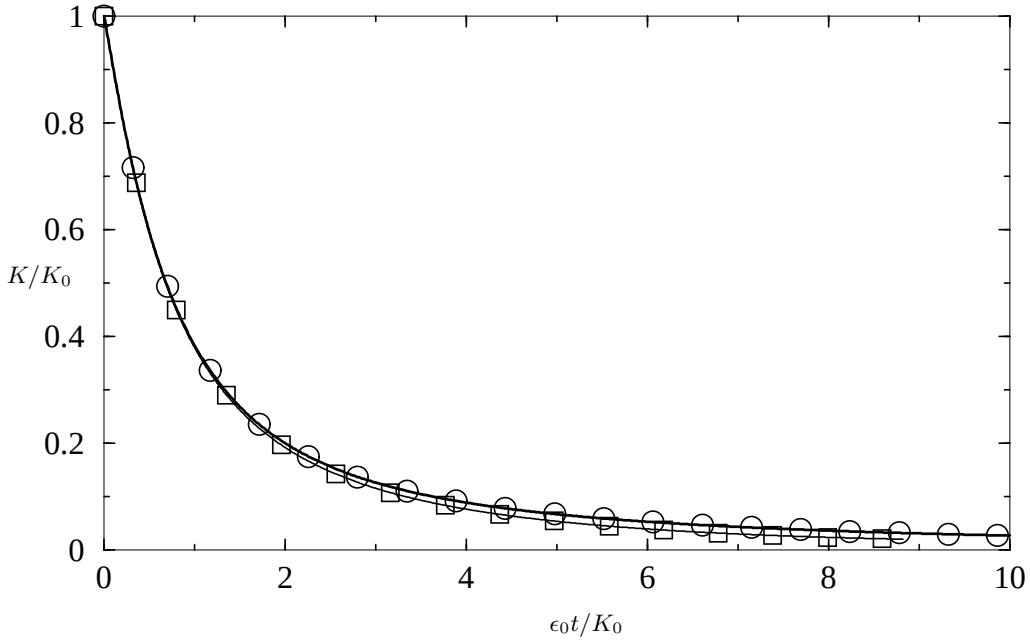

FIGURE 2. Evolution of the normalized turbulent kinetic energy K/K_0 in unsheared stratified turbulence with initial Froude numbers 64 (○) and 6.4 (□).

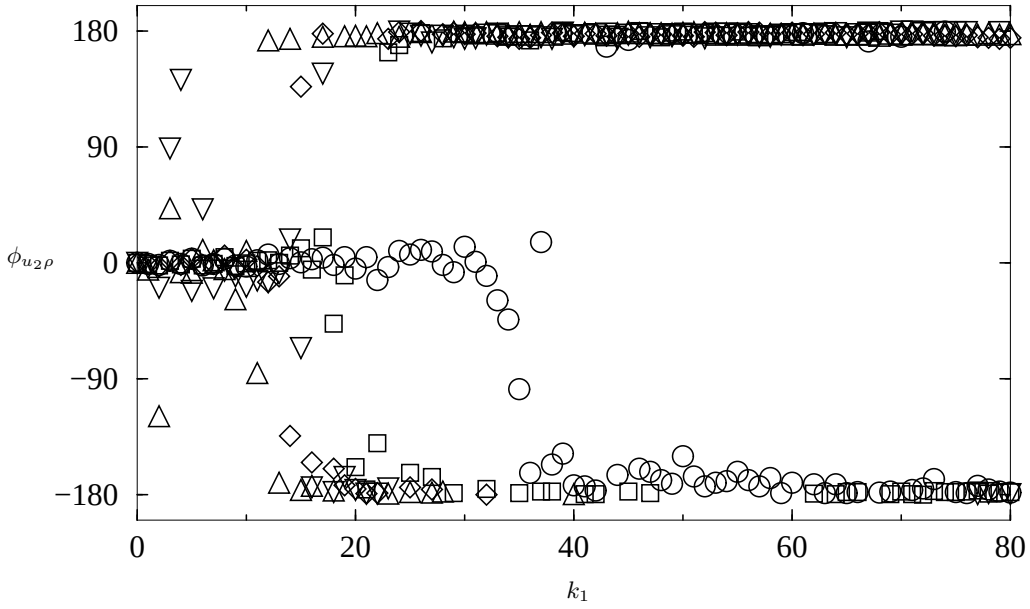

FIGURE 3. Spectrum of the phase angle $\phi_{u_2\rho}$ in sheared stratified turbulence at $St = 5$ with Richardson numbers 0 (○), 0.1 (□), 0.2 (◇), 0.5 (△), and 1.0 (▽).

where $Fr = \sqrt{\overline{u_2^2}}/(LN)$. A slightly stronger decay of the turbulent kinetic energy is found for the more strongly-stratified simulation.

3. Phase angle in sheared stably stratified turbulence

In this section, the phase angle in sheared stably-stratified turbulence is discussed. The Richardson number Ri is varied from $Ri = 0$, corresponding to unstratified shear flow, to $Ri = 1$, corresponding to strongly-stratified shear flow.

Figure 3 shows the spectrum of the phase angle $\phi_{u_2\rho}$ between the vertical velocity u_2 and the density ρ at non-dimensional time $St = 5$. In the unstratified simulation with $Ri = 0$ (○ symbols), phase angles $\phi_{u_2\rho} \approx 0$ are found for small wavenumbers k_1, and phase angles $\phi_{u_2\rho} \approx \pm 180^\circ$ are found for large values of k_1. The transition from $\phi_{u_2\rho} \approx 0$ to $\phi_{u_2\rho} \approx \pm 180^\circ$ occurs at a wavenumber $k_1 \approx 35$. At this wavenumber, the cospectrum $Co_{u_2\rho}$ crosses zero and changes sign. As the Richardson number is increased, the transition wavenumber decreases to about $k_1 \approx 20$ for $Ri = 0.1$, $k_1 \approx 17$ for $Ri = 0.2$, $k_1 \approx 10$ for $Ri = 0.5$, and $k_1 \approx 5$ for $Ri = 1$. Phase angles $\phi_{u_2\rho} \approx \pm 90^\circ$, indicating possible internal wave motion, are observed only in the strongly stratified simulations with $Ri = 0.5$ and $Ri = 1$ and only for a few scattered wavenumbers, not over a region of wave-space. Again, these isolated instances of 90° phase angles are associated with zero-crossings of the associated cospectrum, rather than a region in wavespace exhibiting wavelike behavior.

Figure 4 shows the probability distribution of the phase angle $\phi_{u_2\rho}$ over an instantaneous flow field. The phase angle distribution of the unstratified simulation with $Ri = 0$ has a slight maximum at $\phi_{u_2\rho} = 0$, indicating a very modest predominance of down-gradient mixing. As the Richardson number is increased, the maximum of the phase angle distribution is found at $\phi_{u_2\rho} = \pm 180^\circ$, corresponding to counter-gradient mixing.

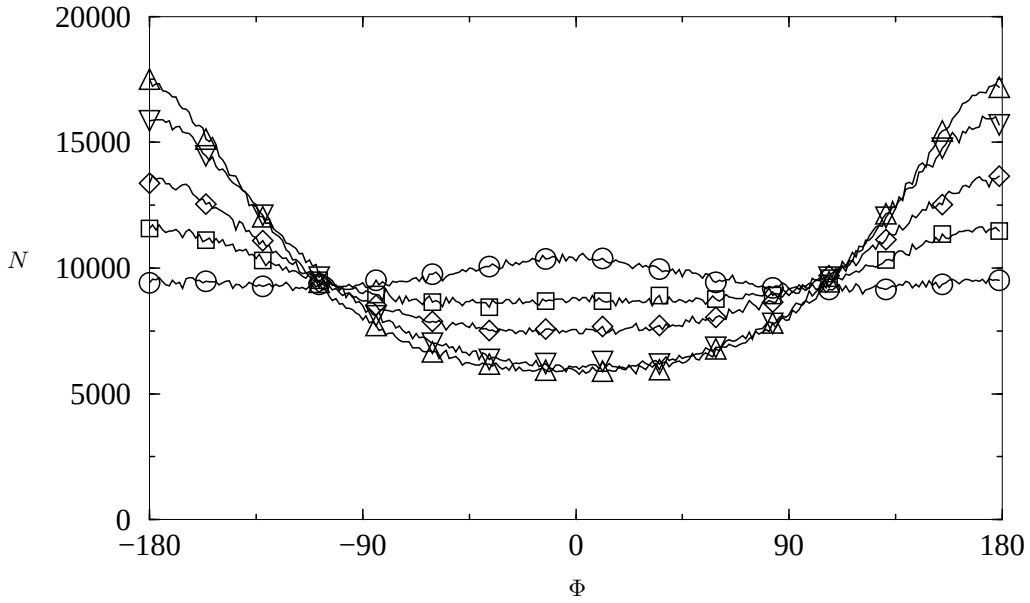

FIGURE 4. Distribution of the phase angle $\phi_{u_2\rho}$ in sheared stratified turbulence at $St = 5$ with Richardson numbers 0 (○), 0.1 (□), 0.2 (◇), 0.5 (△), and 1.0 (▽).

The largest contribution to $\phi_{u_2\rho} = \pm 180°$ is found in the $Ri = 0.5$ case, which also shows the strongest counter-gradient mixing coefficient. For all cases, a continuous phase angle distribution is observed. There are no local peaks apparent around $\phi_{u_2\rho} = \pm 90°$ that would suggest regions of wavelike behavior distinct from the background turbulence.

In order to obtain a more complete picture of phase angle distributions in turbulent stratified flow, figure 5 shows the distribution of the phase angle $\phi_{u_1u_2}$ between downstream, u_1, and vertical, u_2, velocity components, again at $St = 5$. The distribution is relatively unaffected by the Richardson-number variation. It shows strong peaks around $\phi_{u_1u_2} = 0$ and around $\phi_{u_1u_2} = \pm 180°$ that can be explained using the continuity equation. For modes with $k_3 = 0$, the continuity equation in wave space requires that the Fourier coefficients $\tilde{u}_1$ and $\tilde{u}_2$ are in the same direction, corresponding to $\phi_{u_1u_2} = 0$, or in opposite directions, corresponding to $\phi_{u_1u_2} = \pm 180°$. The peaks are therefore a result of two-dimensional modes.

4. Phase angle in unsheared stably-stratified turbulence

In this section, the phase angle in unsheared decaying stably stratified turbulence is discussed. A weakly-stratified case with initial Froude number $Fr = 64$ is compared to a more strongly stratified case with $Fr = 6.4$.

The spectrum of the phase angle $\phi_{u_2\rho}$ after about 10 eddy-turnover times is shown in figure 6. The weakly-stratified case with $Fr = 64$ has $\phi_{u_2\rho} \approx 0$ for all k_1, corresponding to down-gradient flux. The case with $Fr = 6.4$, however, shows $\phi_{u_2\rho} \approx \pm 180°$ for wave numbers larger than about $k_1 = 30$, corresponding to counter-gradient mixing. As in the sheared cases, there is no band in wavespace with wavelike behavior.

The phase-angle distribution over the instantaneous field at the same time as in figure 6 is shown in figure 7. The distribution in the weakly-stratified case shows a clear maximum

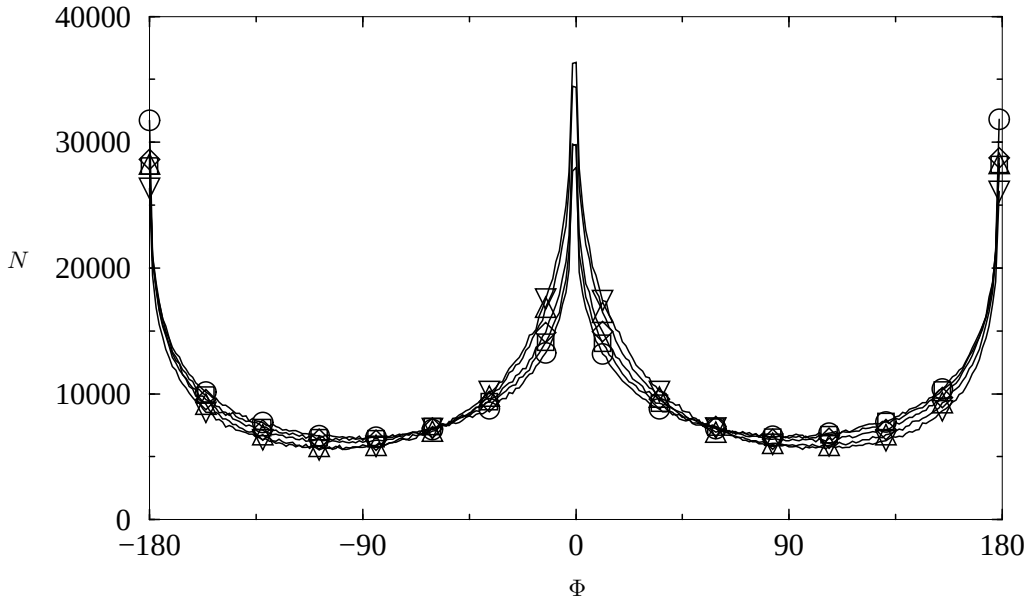

FIGURE 5. Distribution of the phase angle $\phi_{u_1u_2}$ in sheared stratified turbulence at $St = 5$ with Richardson numbers 0 (○), 0.1 (□), 0.2 (◇), 0.5 (△), and 1.0 (▽).

around $\phi_{u_2\rho} = 0$. However, the phase angles are widely distributed, which perhaps would not have been anticipated given the distribution in figure 6, which shows averaged phase angles at a given wavenumber. The distribution in the $Fr = 6.4$ case shows a maximum around $\phi_{u_2\rho} = \pm 180°$, corresponding to counter-gradient mixing. The distribution of phase angles between downstream velocity u_1 and vertical velocity u_2 is very similar to that of the sheared case, with strong peaks at 0° and ±180° and a weak dependence on the strength of the stratification.

5. Normal-mode analysis

A normal-mode analysis of the linearized inviscid equations of motion for the unsheared flow is performed. The direct numerical simulation results are then projected onto the eigensolution in order to extract a possible linear wave motion present in these results .

The analysis is based on the following linearized inviscid equations of motion:

$$\frac{\partial \rho}{\partial t} = -S_\rho u_2$$

$$\frac{\partial u_i}{\partial t} = -\frac{1}{\rho_0}\frac{\partial p}{\partial x_i} - \frac{g}{\rho_0}\rho\delta_{i2}$$

The pressure is eliminated from the equations using the continuity equation. The equations are transformed into Fourier space and take the following form:

$$\frac{\partial \tilde{\rho}}{\partial t} = -\frac{g}{\rho_0}S_\rho \tilde{u}_2 = N^2\tilde{u}_2$$

$$\frac{\partial \tilde{u}_i}{\partial t} = \tilde{\rho}\left(\frac{k_i k_2}{k^2} - \delta_{i2}\right) .$$

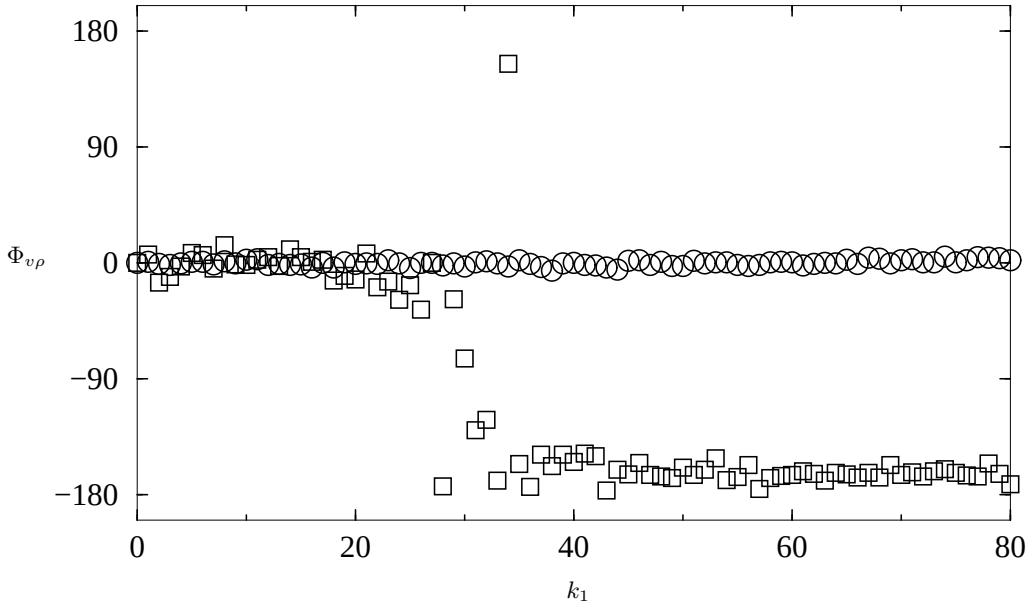

FIGURE 6. Spectrum of the phase angle $\phi_{u_2\rho}$ in unsheared stratified turbulence after about 10 eddy-turnover times with initial Froude numbers 64 (○) and 6.4 (□).

Normal modes of the form

$$\begin{pmatrix} \tilde{\rho} \\ \tilde{u}_1 \\ \tilde{u}_2 \\ \tilde{u}_3 \end{pmatrix} = \begin{pmatrix} \hat{\rho} \\ \hat{u}_1 \\ \hat{u}_2 \\ \hat{u}_3 \end{pmatrix} \exp i(k_j x_j + \omega t)$$

are introduced and lead to the following system of equations:

$$\begin{pmatrix} i\omega & 0 & S_\rho & 0 \\ -\frac{g}{\rho_0}\frac{k_1 k_2}{k^2} & i\omega & 0 & 0 \\ -\frac{g}{\rho_0}\left(\frac{k_2^2}{k^2}-1\right) & 0 & i\omega & 0 \\ -\frac{g}{\rho_0}\frac{k_2 k_3}{k^2} & 0 & 0 & i\omega \end{pmatrix} \begin{pmatrix} \hat{\rho} \\ \hat{u}_1 \\ \hat{u}_2 \\ \hat{u}_3 \end{pmatrix} = 0$$

From this system of equations, the following dispersion relation is obtained:

$$\omega^2 = 0 \qquad \omega = \pm\sqrt{D}$$

Here, D takes the following value:

$$D = N^2 \frac{k_1^2 + k_3^2}{k^2}$$

The following eigenvectors are obtained:

$$\mathbf{e}_{1,3} = \begin{pmatrix} S_\rho(k_1^2+k_3^2) \\ \mp i k_1 k_2 \sqrt{D} \\ \pm i(k_1^2+k_3^2)\sqrt{D} \\ \mp i k_2 k_3 \sqrt{D} \end{pmatrix} \qquad \mathbf{e}_2 = \begin{pmatrix} 0 \\ 1 \\ 0 \\ 0 \end{pmatrix} \qquad \mathbf{e}_4 = \begin{pmatrix} 0 \\ 0 \\ 0 \\ 1 \end{pmatrix}$$

The solution from direct numerical simulations can now be expressed in terms of the

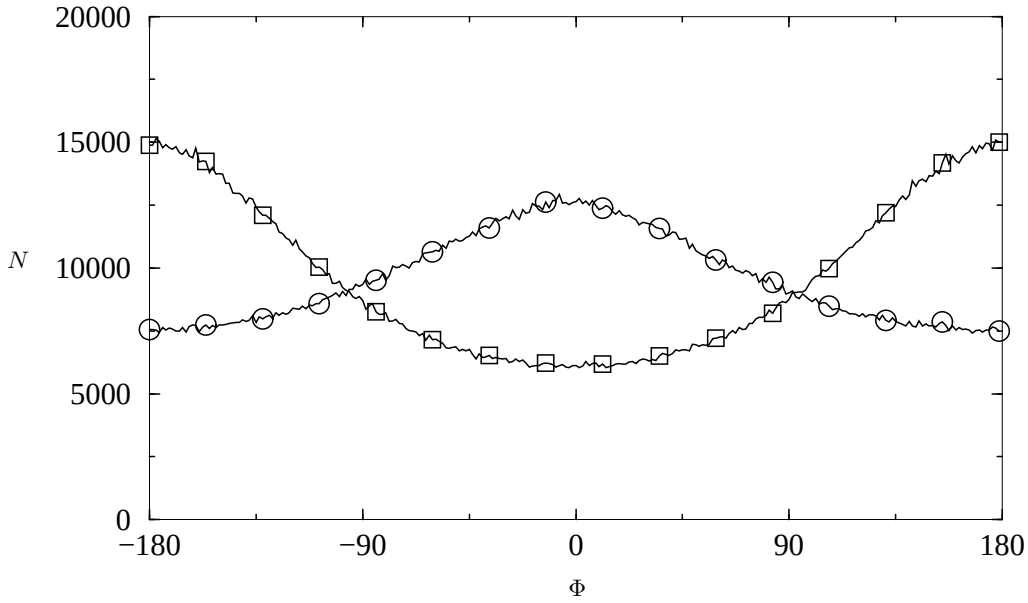

FIGURE 7. Distribution of the phase angle $\phi_{u_2\rho}$ in unsheared stratified turbulence after about 10 eddy-turnover times with initial Froude numbers 64 (○) and 6.4 (□).

eigenvectors:

$$\mathbf{a}_{DNS} = a_1\mathbf{e}_1 + a_2\mathbf{e}_2 + a_3\mathbf{e}_3 + a_4\mathbf{e}_4$$

Here, the components a_2 and a_4 describe horizontal vortical motion. The components a_1 and a_3 define an upper bound for the wave motion present in the field. Note that any DNS data, except that for k_1 and k_3 both zero, can be represented by a choice of complex a_1, a_2, a_3, and a_4. The coefficients are found by multiplication with the complex conjugate of the eigenvectors of the adjoint problem.

Note that the solution to the linearized governing equations is also used in Rapid Distortion Theory. The analytical solution to the equations presented at the beginning of this section was developed by Hanazaki and Hunt (1996). The solutions of these linearized equations show an impressive degree of similarity to solutions of the full nonlinear problem and capture much of the distinctive behavior of stably-stratified turbulence. Remarkably, Hanazaki and Hunt (2002) have extended this analysis to include the case of uniformly-sheared stratified turbulence as well. Presumably this solution could be used to provide guidance on how to decompose the sheared flow fields, but the difficulties encountered above would still be present (that is, all of the turbulent motion could be represented by the eigenvectors of the linearized system and, even after eliminating horizontal motions containing the vertical vorticity, the remaining "wave" motion could still contain a turbulent component).

6. Summary

In this study, the phase angle $\phi_{u_2\rho}$ between vertical velocity u_2 and density ρ was computed from direct numerical simulations of sheared and unsheared homogeneous stratified turbulence. A broad distribution of the phase angle was found that is consistent with

the observed down-gradient mixing for weakly stratified flow and counter-gradient mixing for strongly stratified flow. However, the broad distribution hides any internal wave signature that may be present in the flow.

A decomposition based on linear analysis has been proposed for unsheared decaying stratified turbulence. The flow fields are decomposed into horizontal vortical motions and vertical wave motions. However, there may still be some turbulent motion contained in the wave field. In agreement with Stewart (1969) we find that "there is probably no really clear-cut distinction between turbulence and waves".

REFERENCES

Briggs, D. A., Ferziger, J. H., Koseff, J. R. & Monismith, S. G. 1998 Turbulent mixing in a shear-free stably stratified two-layer fluid. *J. Fluid Mech.* **354**, 175–208.

Craya, A. 1958 Contribution à l'analyse de la turbulence associée à des vitesses moyennes. Pub. Sci et Tech. du Ministère de l'Air (France) No. 345.

Ertel, H. 1942 Ein neuer hydrodynamischer Wirbelsatz. Meteorol. Z., **59**, 271–281.

Gerz, T., Schumann, U. & Elghobashi, S. E. 1989 Direct numerical simulation of stratified homogeneous turbulent shear flows. *J. Fluid Mech.* **200**, 563–594.

Hanazaki, H. & Hunt, J. C. R. 1996 Linear processes in unsteady stably stratified turbulence. *J. Fluid Mech.* **318**, 303–337.

Hanazaki, H. & Hunt, J. C. R. 2002 Structure of unsteady stably stratified turbulence with mean shear. Submitted to J. Fluid Mech.

Herring, J. R. & Métais, O. 1989 Numerical experiments in forced stably stratified turbulence. *J. Fluid Mech.* **202**, 97–115.

Holt, S. E., Koseff, J. R. & Ferziger, J. H. 1992 A numerical study of the evolution and structure of homogeneous stably stratified sheared turbulence. *J. Fluid Mech.* **237**, 499–539.

Jacobitz, F. G., Sarkar, S. & Van Atta, C. W. 1997 Direct numerical simulations of the turbulence evolution in a uniformly sheared and stably stratified flow. *J. Fluid Mech.* **342**, 231–261.

Jacobitz, F. G. 2000 Scalar transport and mixing in turbulent stratified shear flow. *Int. J. Heat Fluid Flow* **21**, 535–541.

Komori, S., Ueda, H., Ogino, F. & Mizushina, T. 1983 Turbulence structure in stably stratified open-channel flow. *J. Fluid Mech.* **130**, 13–26.

Lienhard, J. H. & Van Atta, C. W. 1990 The decay of turbulence in thermally stratified flow. *J. Fluid Mech.* **210**, 57–112.

McBean, G. A. & Miyake, M. (1972) Turbulent transfer mechanisms in the atmospheric surface layer. *Quart. J. R. Met. Soc.* **98**, 383–398.

Métais, O. & Herring, J. R. 1989 Numerical simulations of freely evolving turbulence in stably stratified fluids. *J. Fluid Mech.* **202**, 117–148.

Piccirillo, P. S. & Van Atta, C. W. 1997 The evolution of a uniformly sheared thermally stratified turbulent flow. *J. Fluid Mech.* **334**, 61–86.

Riley, J. J., Metcalfe, R. W. & Weissman, M. A. 1981 Direct numerical simulations of homogeneous turbulence in density-stratified fluids. In *Nonlinear Properties of Waves* (B. J. West, ed.), 79–112.

Rohr, J. J., Itsweire, E. C., Helland, K. N. & Van Atta, C. W. 1988 Growth and decay of turbulence in a stably stratified shear flow. *J. Fluid Mech.* **195**, 77–111.

Staquet, C. & Riley, J. J. 1989 On the velocity field associated with potential vorticity. *Dyn. Atmos. and Oceans* **14**, 93–123.

Shih, L.H., Koseff, J.R., Ferziger, J.H. & Rehmann, C.R. 2000 Scaling and parameterization of stratified homogeneous turbulent shear flow. *J. Fluid Mech.* **412**, 1–20.

Stewart, R. W. 1969 Turbulence and waves in a stratified atmosphere. *Radio Sci.* **4**, 1269–1278.

Stillinger, D. C., Helland, K. N. & Van Atta, C. W. 1983 Experiments on the transition of homogeneous turbulence to internal waves in a stratified fluid. *J. Fluid Mech.* **131**, 91–122.

Yoon, K. & Warhaft, Z. 1990 The evolution of grid generated turbulence under conditions of stable thermal stratification. *J. Fluid Mech.* **215**, 601–638.